

Iterative Blind Image Deconvolution in Space and Frequency Domains

Edmund Y. Lam and Joseph W. Goodman

Information Systems Laboratory, Stanford University, Stanford, CA 94305

ABSTRACT

In image acquisition, the captured image is often the result of the object being convolved with a blur function. Deconvolution is necessary in order to undo the effects of the blur. However, in real life we may have very little knowledge of the blur, and therefore we have to perform blind deconvolution. One major challenge of existing iterative algorithms for blind deconvolution is the enforcement of the convolution constraint. In this paper we describe a method whereby this constraint can be much more easily implemented in the frequency domain. This is possible because of Parseval's theorem, which allows us to relate projection in the space and frequency domains. Our algorithm also incorporates regularization of the estimated image through the use of Wiener filters. The restored images are compared to the original and noisy blurred images, and we find that the restoration process indeed provides an enhancement in visual quality.

Keywords: Image restoration, blind deconvolution, projection, digital photography

1. INTRODUCTION

The popularity of digital photography has increased tremendously over the last few years. In addition to facilitating easy transmission and sharing of pictures, digitized photographs also allow us to make use of the ever-increasing computational power available in image post-processing in order to enhance the quality of the final output images. At the same time, this would also impact the design of cameras, as we may sacrifice some precision of the instruments and instead rely on the post-processing to fine-tune the images. For example, we might not need to move the lens to the precise position for focusing, but can correct for the error by digital restoration. Since it is rarely the case that we know exactly the imperfection introduced into the image acquisition system, the challenge is to derive the object as well as the blur directly from only one observation.

In imaging using a diffraction-limited system with incoherent light, the object and the image are related by¹

$$\mathcal{G}_i(f_x, f_y) = \mathcal{H}(f_x, f_y)\mathcal{G}_g(f_x, f_y), \quad (1)$$

where \mathcal{G}_i is the normalized frequency spectrum of the image intensity $i(x, y)$, \mathcal{G}_g is the normalized frequency spectrum of the object intensity $g(x, y)$, and \mathcal{H} is called the optical transfer function (OTF). Noise is inevitably present in any imaging system, and is customarily modeled as additive white Gaussian noise at the output. Taking equation (1) to the space domain by inverse Fourier transforms, and including the contribution of noise, we have the convolution equation

$$i(x, y) = h(x, y) * g(x, y) + n(x, y), \quad (2)$$

where $h(x, y)$ is the inverse Fourier transform of $\mathcal{H}(f_x, f_y)$, and $n(x, y)$ is the additive noise. Our deblurring challenge is therefore a blind deconvolution problem, where we seek to deconvolve our observation $i(x, y)$ to obtain a close approximation to the object $g(x, y)$ without an exact knowledge of the degradation $h(x, y)$.

2. EXISTING APPROACHES

In the absence of noise, it has been shown that the blind deconvolution problem almost always has a unique solution even without any prior knowledge of the blur or the object.² This is easiest to comprehend if we take the z -transform of equation (2) while neglecting the noise term and obtain

$$I(z_1, z_2) = H(z_1, z_2)G(z_1, z_2). \quad (3)$$

The blind deconvolution problem can now be cast as a factorization problem: given a bi-variate polynomial $I(z_1, z_2)$, factorize it into two components $H(z_1, z_2)$ and $G(z_1, z_2)$, neither of which is a constant. While this factorization is not unique for one-dimensional signals because of the fundamental theorem of algebra*, it is unique for higher dimensions up to a scaling factor except for contrived cases. Such factorization can theoretically be obtained by looking at the zero-sheets of $I(z_1, z_2)$; for more information and algorithms, the reader is referred to Refs. 3–5.

Unfortunately, all imaging systems contain noise, and they affect the unique factorization property in a non-trivial way. Almost always $I(z_1, z_2)$ becomes not factorizable. If we seek only approximate solutions, they may not be unique. Furthermore, zero-sheets are neither easy to visualize (since they are two-dimensional surfaces in a four-dimensional space) nor efficient to compute. For instance, the algorithm provided in Ref. 4 has a complexity of $O(N^4)$ for an image of size $N \times N$, which creates a major problem as the image resolution in typical digital photographs continues to rise rapidly.

Instead of this purely algebraic approach, most existing blind deconvolution algorithms are iterative in nature. They have a common structure as follows^{6–8}:

1. Find an initial guess of the image g ;
2. From this initial guess deduce the point-spread function h , imposing constraints on h such as positivity and finite support;
3. From the new h , deduce the next estimate of the image g , imposing constraints on g such as positivity and finite support;
4. Go back to 2 and iterate.

The major challenge in these iterative algorithms lies in the enforcement of the convolution constraint. For example, we may be required to solve a large constrained least-square system, and need an effective pre-conditioning algorithm for the matrices because the restoration problem is inherently ill-conditioned.⁹

We believe, however, that the convolution constraint can be more naturally and efficiently implemented in the frequency domain. Furthermore, the OTF is bandlimited for an incoherent imaging system,¹ which is also a frequency domain constraint. In section 3, we describe a method that takes advantage of the availability of both space and frequency domains.

3. ALGORITHM

3.1. POCS

The motivation for our blind image deconvolution algorithm comes from projection onto convex sets (POCS), which is a powerful signal reconstruction technique.^{10,11} We define constraints, such as positivity and finite support, on the object and the blur function. As long as all constraints involve convex sets, the fundamental theorem of POCS guarantees a weak convergence to a fixed point in the intersection of the sets provided that it exists. Ref. 12 provides a detailed tutorial on POCS, its extensions, and some applications.

As with Ref. 13, we operate on a Hilbert space of function pairs, $\mathcal{H} = \{(s, t) : s \in l^2, t \in l^2\}$, with the inner product defined as

$$\langle (s, t), (u, v) \rangle \triangleq \left(\sum_{\zeta} s(\zeta)u(\zeta) + \sum_{\eta} t(\eta)v(\eta) \right). \quad (4)$$

The induced norm is, as usual,

$$\|(s, t)\| \triangleq \sqrt{\langle (s, t), (s, t) \rangle}. \quad (5)$$

*The fundamental theorem of algebra states that any polynomial of degree n can be factorized as $p(z) = c \prod_{i=1}^n (z - z_i)$, where c is a constant and z_i 's are the roots. Therefore, to factorize $p(z)$ into 2 components, there are many possibilities even if we ignore the constant c .

It is easy to verify that this satisfies the usual requirements of a norm.¹⁴ After defining the Hilbert space, next we need to specify the three basic sets of constraints for the blind deconvolution problem:

1. $\mathcal{C}_g \triangleq \{(s, t) : s \text{ satisfying prescribed prior knowledge about the object } g\}$,
2. $\mathcal{C}_h \triangleq \{(s, t) : t \text{ satisfying prescribed prior knowledge about the point-spread function } h\}$, and
3. $\mathcal{C}_i \triangleq \{(s, t) : s * t = i\}$.

The POCS algorithm can be compactly written as¹³

$$(g, h)_{(k+1)} = \mathcal{P}_i \mathcal{P}_h \mathcal{P}_g (g, h)_k \quad k = 0, 1, 2, \dots \quad (6)$$

where \mathcal{P} denotes the projection onto the corresponding set, and the subscript k is the index of iteration. Projection \mathcal{P} from a point x to a set \mathcal{C} is done by finding the point $y \in \mathcal{C}$ such that $\|x - y\|$ is minimum. The existence of a unique point y is guaranteed for convex sets in a Hilbert space.¹⁵ Furthermore, weak convergence still holds if we relax the projection operator \mathcal{P} to $\mathcal{T} = I + \lambda(\mathcal{P} - I)$, with $\lambda \in (0, 2)$. This added flexibility sometimes help in accelerating the rate of convergence.¹²

3.2. Frequency Domain Projection

\mathcal{C}_g and \mathcal{C}_h define simple convex sets with projection operators that are both easy to calculate and implement. \mathcal{C}_i , however, is not jointly convex in (s, t) . For example, if $s_0 * t_0 = i$, then $\frac{1}{2}s_0 * 2t_0 = i$, but $\frac{3}{4}s_0 * \frac{3}{2}t_0 \neq i$. This violates the condition for a convex set, in which the midpoint of any two points in the set should also be in the set. Nevertheless, we may still be able to find \mathcal{P}_i , although it is usually much more difficult to evaluate, and could involve solving a set of nonlinear equations.¹³

Yet, if we write the convolution relationship in the spatial frequency domain, the expressions are much simpler to evaluate. We replace \mathcal{C}_i by $\mathcal{C}_I \triangleq \{(S, T) : S \cdot T = I\}$ where the capital letters refer to signals in the frequency domain, and “ \cdot ” represents entrywise multiplication. Our goal is to perform the projection in the frequency domain directly, which would offer us the following advantages:

1. The projection operator is much simpler. Rather than dealing with a large system of convolution in spatial domain, in frequency domain each frequency component is decoupled from all others, and we can perform the projection successively in each frequency. This also allows the algorithmic complexity to scale reasonably with image size.
2. As in Ref. 13, we can combine \mathcal{C}_g and \mathcal{C}_h into one convex set and therefore, for projection with only two sets, the summed distance error reduction property holds even though one of the sets is non-convex.¹⁶
3. It is easier to tackle the problem of additive noise with the use of Wiener filtering, as we will demonstrate in section 3.3.

It is extremely important to realize that \mathcal{C}_I lies in another Hilbert space with a norm that is different from (5). In general, for such cases the theory of POCS may not hold, as reduction in distance in one space does not automatically imply a decrease in distance in another. Fortunately, for a Fourier pair, Parseval’s theorem in the discrete domain states that

$$\sum |s(x, y)|^2 = \frac{1}{N^2} \sum |S(f_x, f_y)|^2, \quad (7)$$

so the norms in the two Hilbert spaces are proportional. Therefore, reduction in distance in one domain indeed carries through to the other domain as well. However, this dependence on Parseval’s theorem does limit the extension of the algorithm, as for example, a weighted norm in the space domain has no equivalence in the frequency domain.

3.3. Regularization

It is well-known that the image deconvolution problem is ill-posed in the continuous domain and ill-conditioned in the discrete domain. The problem is even worse for blind deconvolution, where we also have uncertainty in the deconvolution operator. Regularization is therefore essential for visually pleasant output images.

There are many different regularization methods commonly used in image deconvolution, such as Tikhonov-Miller regularization,¹⁷ constrained least-squares (CLS),¹⁸ and early termination.¹⁹ Except for early termination, most of the methods are implemented in the space domain. Since the main effect of regularization is the suppression of high frequency contents, it is seen that Wiener filtering achieves similar results.²⁰ Furthermore, we will show that Wiener filtering is also consistent with our projection idea.

In traditional Wiener filtering, if the blur function $h(x, y)$ is known, the object is estimated by:¹

$$\hat{G}(f_x, f_y) = \frac{H^*(f_x, f_y)}{|H(f_x, f_y)|^2 + \frac{\Phi_n(f_x, f_y)}{\Phi_g(f_x, f_y)}} I(f_x, f_y), \quad (8)$$

where Φ_n and Φ_g denote the power spectra of the noise and object respectively. Note that for low frequencies, we typically have the noise spectrum much smaller than the signal spectrum, and hence Φ_n/Φ_g is close to zero. In that case, the Wiener filter is approximately an inverse filter. On the other hand, for high frequencies, the noise spectrum remains the same since we have white noise, and it will usually far exceed the signal spectrum. Therefore, Φ_n/Φ_g would dominate both $|H|^2$ and H^* , making the Wiener filter approximately zero. The Wiener filter therefore regulates the amount of high frequency content possible.

At the same time, we can interpret Wiener filtering in terms of a minimum-norm projection. For the moment we turn the object, image, and noise to vectors by means of lexicographic ordering. The vectors can be considered to reside in a vector space with inner product $\langle \mathbf{x}, \mathbf{y} \rangle \triangleq E[\mathbf{xy}]$, where E denotes expectation. Again, it can be verified that this is a valid inner product, even though it is not a scalar.²¹ Therefore, we can ask for the projection of the object vector \mathbf{g} onto the space generated by the observed image vector \mathbf{i} . Let the projection be $\hat{\mathbf{g}} = K\mathbf{i}$. By the orthogonality relationship,

$$\langle \mathbf{g} - K\mathbf{i}, \mathbf{i} \rangle = 0. \quad (9)$$

After rearranging the terms, we get

$$K = E[\mathbf{gi}]E[\mathbf{ii}]^{-1}. \quad (10)$$

The Fourier transform of the image equivalence of K is seen to be¹⁸

$$K(f_x, f_y) = \frac{H^*(f_x, f_y)\Phi_g(f_x, f_y)}{|H(f_x, f_y)|^2\Phi_g(f_x, f_y) + \Phi_n(f_x, f_y)} = \frac{H^*(f_x, f_y)}{|H(f_x, f_y)|^2 + \frac{\Phi_n(f_x, f_y)}{\Phi_g(f_x, f_y)}}, \quad (11)$$

which is exactly the form in equation (8).

Note that Φ_n and Φ_g are unknowns for blind deconvolution. Φ_n can be measured by some noise-estimation algorithms. As for Φ_g , since

$$\Phi_i = |H|^2\Phi_g + \Phi_n, \quad (12)$$

we could estimate Φ_g by using Φ_i and Φ_n , which can both be estimated at the beginning of the algorithm, together with the current estimate of H . Alternatively, one could replace Φ_n/Φ_g by the noise-to-signal ratio. Implicitly in this setting, we are assuming that the signal is also white, hence the spectrum is a constant just like the noise spectrum. In that case, the Wiener filter is also called the pseudo-inverse filter.²⁰ Although this assumption is not accurate, the resulting images are often of sufficiently good quality.

Therefore, for our regularized projection of the convolution operation, we have the following simultaneous projection:

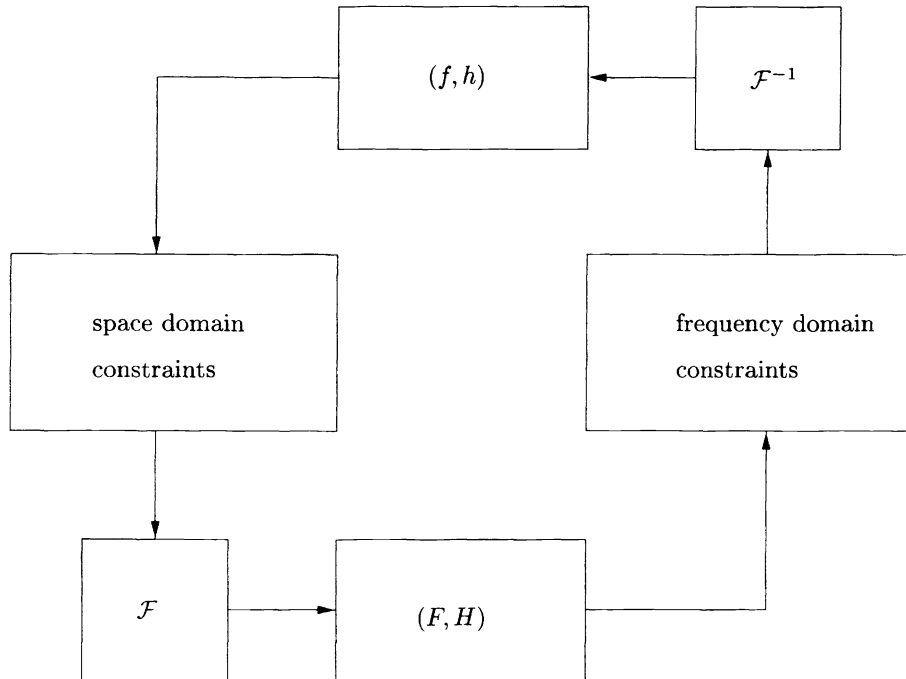


Figure 1: Alternating Minimization Algorithm

$$G^{(k+1)}(f_x, f_y) = \frac{H^{(k)*}(f_x, f_y)}{|H^{(k)}(f_x, f_y)|^2 + \frac{\Phi_n(f_x, f_y)}{\Phi_g^{(k)}(f_x, f_y)}} I(f_x, f_y) \quad (13)$$

$$H^{(k+1)}(f_x, f_y) = \frac{G^{(k)*}(f_x, f_y)}{|G^{(k)}(f_x, f_y)|^2 + \frac{\Phi_n(f_x, f_y)}{\Phi_h^{(k)}(f_x, f_y)}} I(f_x, f_y), \quad (14)$$

where the superscript (k) denotes the variable at the k th iteration. Our blind deconvolution algorithm is summarized in figure 1.

4. SIMULATION

We take the image “baboon” shown in figure 2 from the standard image processing library for simulation. The size of the image is 256×256 . This image is subjected to a space-invariant out-of-focus blur, with the severity parameter $W_m/\lambda = 0.5$.^{1,22} Since the system is bandlimited, the blur cannot be space-limited. Instead, we decided that the majority of the non-zero components are in the center 13×13 pixels, so we use that as the support size of the blur. No other information about the blur is provided to the algorithm, however, except that it is circularly symmetric. A white Gaussian noise is also added to the blur image, with a signal-to-noise ratio of about 30dB. Initially, we take an impulse as the estimate for the blur, and the observed blurred image as the first guess for the image. Also, a constant noise-to-signal ratio is used in place of Φ_n/Φ_g .

Figure 3 shows the noisy blurred image on the left, and the blindly restored image on the right after 20 iterations of the proposed algorithm. We can see that indeed the restored image has closer resemblance to the original image than the blurred image, as some of the high frequency components have been restored. Moreover, it demonstrates that modeling the out-of-focus blur which is not space-limited by a blur of small finite support does not significantly hamper the effectiveness of the algorithm.

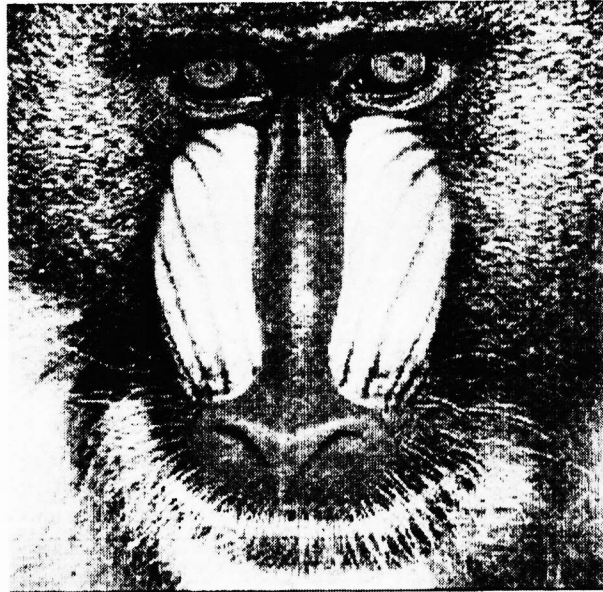


Figure 2: "Baboon" test image



(a) Blurred image



(b) Restored image

Figure 3: Restoration of blurred "baboon" image

5. CONCLUSIONS

In this paper we have demonstrated a novel projection-based algorithm for blind deconvolution. We show how the convolution constraint can be better implemented in the frequency domain, and how regularization can be naturally incorporated through the use of Wiener filtering. Note that throughout the paper, we have assumed that the only knowledge of the blur is circular symmetry. If we have more *a priori* information on the blur, we can add other constraint sets and they should help us arrive at a better image. As long as the new sets are convex, they can be combined with \mathcal{C}_g and \mathcal{C}_h to form smaller convex sets and the algorithm continues to be applicable.

ACKNOWLEDGMENTS

This work is partially supported under the Programmable Digital Camera project by Intel, Hewlett-Packard, Kodak, Canon, and Interval Research.

REFERENCES

1. J. W. Goodman, *Introduction to Fourier Optics*, McGraw-Hill, New York, second ed., 1996.
2. R. Bates and H. Jiang, "Blind deconvolution — recovering the seemingly irrecoverable!," in *International Trends in Optics*, J. W. Goodman, ed., pp. 423–437, 1991.
3. R. Bates, B. Quek, and C. Parker, "Some implications of zero sheets for blind deconvolution and phase retrieval," *Journal of the Optical Society of America A* **7**, pp. 468–479, March 1990.
4. D. Ghiglia, L. Romero, and G. Mastin, "Systematic approach to two-dimensional blind deconvolution by zero-sheet separation," *Journal of the Optical Society of America A* **10**, pp. 1024–1036, May 1993.
5. P. Bones, C. Parker, B. Satherley, and R. Watson, "Deconvolution and phase retrieval with use of zero sheets," *Journal of the Optical Society of America A* **12**, pp. 1842–57, September 1995.
6. G. Ayers and J. Dainty, "Iterative blind deconvolution method and its applications," *Optics Letters* **13**, pp. 547–549, July 1988.
7. Y.-L. You and M. Kaveh, "A regularization approach to joint blur identification and image restoration," *IEEE Transactions on Image Processing* **5**, pp. 416–428, March 1996.
8. T. Chan and C.-K. Wong, "Total variation blind deconvolution," *IEEE Transactions on Image Processing* **7**, pp. 370–375, March 1998.
9. J. G. Nagy, R. J. Plemmons, and T. C. Torgersen, "Iterative image restoration using approximate inverse preconditioning," *IEEE Transactions on Image Processing* **5**, pp. 1151–1162, July 1996.
10. D. C. Youla and H. Webb, "Image restoration by the method of convex projections: Part 1 — theory," *IEEE Transactions on Medical Imaging* **MI-1**, pp. 81–94, October 1982.
11. M. Sezan and H. Stark, "Image restoration by the method of convex projections: Part 2 — applications and numerical results," *IEEE Transactions on Medical Imaging* **MI-1**, pp. 95–101, October 1982.
12. H. Stark and Y. Yang, *Vector Space Projections: A Numerical Approach to Signal and Image Processing, Neural Nets, and Optics*, Wiley, 1998.
13. Y. Yang, N. P. Galatsanos, and H. Stark, "Projection-based blind deconvolution," *Journal of the Optical Society of America A* **11**, pp. 2401–2409, September 1994.
14. W. Rudin, *Principles of Mathematical Analysis*, McGraw-Hill, New York, third ed., 1976.
15. D. G. Luenberger, *Optimization by Vector Space Methods*, Wiley, New York, 1969.
16. A. Levi and H. Stark, "Image restoration by the method of generalized projections with applications to restoration from magnitude," *Journal of the Optical Society of America A* **1**, pp. 932–943, September 1984.
17. A. N. Tikhonov and V. Y. Arsenin, *Solutions of ill-posed problems*, Winston, 1977.
18. H. Andrews and B. Hunt, *Digital Image Restoration*, Prentice Hall, Englewood Cliffs, New Jersey, 1977.
19. D. Kundur and D. Hatzinakos, "A novel blind deconvolution scheme for image restoration using recursive filtering," *IEEE Transactions on Signal Processing* **46**, pp. 375–390, February 1998.
20. K. R. Castleman, *Digital Image Processing*, Prentice Hall, Englewood Cliffs, New Jersey, 1996.
21. T. Kailath, *Lectures on Wiener and Kalman Filtering*, Springer-Verlag, New York, 1981.
22. E. Y. Lam and J. W. Goodman, "Discrete cosine transform domain restoration of defocused images," *Applied Optics* **37**, pp. 6213–6218, September 1998.